Available online at www.sciencedirect.com
SCIENCE DIRECT
Journal of Asian Earth Sciences 28 (2006) 119–132
Journal of Asian Earth Sciences
www.elsevier.com/locate/jaes

The neodymium isotopic and geochemical composition of serpentinites from ophiolitic assemblages in the Qilian fold belt, northwest China

Alan D. Smith*, Houng-Yi Yang

Department of Earth Sciences, Cheng Kung University, Tainan, Taiwan, ROC

Received 5 July 2003; received in revised form 22 January 2004; accepted 14 September 2005

Abstract

Serpentinites are a common component of ophiolitic assemblages in the Qilian fold belt. Samples associated with MORB-like basalts in the northern low-grade blueschist belt of the North Qilian terrane have lherzolitic and pyroxenitic compositions, high $\varepsilon_{Nd}(T)$ values of +5.5 to +6.9, and likely represent residues from melting along spreading ridge segments. Despite evidence for incompatible element enrichment by hydrothermal fluids which had interacted with the ocean floor sediment pile, samples at the Ayougou locality retain original isotope Sm–Nd systematics and yield a Silurian age of 422 ± 20 Ma with $\varepsilon_{Nd}(T) = +6.8$. Serpentinites in the southern high-grade blueschist belt of the North Qilian terrane and from the Lha-Jyi terrane of the South/Central Qilian belt are associated with volcanic arc rocks, and include lherzolitic, harzburgitic and dunitic compositions characterised by low $\varepsilon_{Nd}(T)$ values of +3.8 to −2.2. Harzburgitic samples from these localities display U-shaped REE profiles, and weakly developed negative Nb-anomalies superimposed on incompatible element enrichments, and are interpreted as remnants of oceanic lithosphere metasomatised by slab-derived fluids in a supra-subduction zone environment. Anomalous enrichments in the mobile elements U, Sr and Ba in serpentinites throughout the Qilian belt may be attributed to post-obduction alteration by groundwater.

Keywords: Serpentinites; Trace elements; Nd isotopes; Qilian fold belt

1. Introduction

Serpentinites are a common but little studied component of ophiolitic assemblages in terrane accretion belts despite the geochemical variation in oceanic peridotites being strongly linked to their tectonic origin (e.g. Dick and Bullen, 1984; Bonatti and Michael, 1989; O'Hanley, 1996). Such peridotites are generally agreed to represent residues of melting at ocean ridges, hence their compositional variation should largely reflect the elimination of clinopyroxene on melting (e.g. Elthon, 1992). However, while some peridotites display strongly incompatible element-depleted trace element profiles as would be expected from melt extraction, others are enriched in such elements and have isotopic compositions displaced from depleted mantle values (Prinzhofer and Allègre, 1985; Rampone et al., 1996; Sharma and Wasserburg, 1996). Such features are unlikely to be the result solely of any melt extraction process, and have been ascribed to interaction with fluids during serpentinisation (e.g. Snow et al., 1993; Scambelluri et al., 2001), or in the case of some ophiolitic examples, alteration by groundwater (Gruau et al., 1998). Although serpentinisation is commonly associated with ocean ridges, serpentinites are also common in fore-arc assemblages (e.g. Bloomer, 1983; Johnson and Fryer, 1990; Ballantyne, 1992; Ohara et al., 2002) where they may be related to the invasion of slab-derived fluids into the shallow mantle wedge at temperatures less than 600 °C within the stability field for antigorite (Tatsumi and Eggins, 1995; Hyndman and Peacock, 2003). Determination of the causes of the geochemical features of serpentinites can therefore yield information about the tectonic setting where the rocks underwent alteration and hence their ultimate origin. Considering that most of the constraints on the history of terrane accretion belts is usually gathered from intrusive rocks or sediment sequences which frequently belong to the later stages of basin evolution, it is pertinent to consider what perspective serpentinites can offer. In this study, data is presented for serpentinites from ophiolitic assemblages in the central and northern belts of the Qilian fold belt to illustrate that such rocks can yield significant information despite their severe alteration.

* Corresponding author. Present address: Department of Earth Sciences, University of Durham, Durham, DH1 3LE, UK.
E-mail address: muic2000@yahoo.com (A.D. Smith).

1367-9120/$ - see front matter © 2006 Elsevier Ltd. All rights reserved.
doi:10.1016/j.jseaes.2005.09.013

2. Background and sampling

The Qilian fold belt lies along the southwestern margin of the Sino-Korean craton and has been divided into northern, central, and southern belts (Fig. 1). The belts have also interpreted as accreted terranes (e.g. Xiong and Coney, 1985), although these would undoubtedly be of composite origin as each belt contains varying proportions of high-grade crustal blocks and low-grade ophiolitic assemblages (e.g. Wan et al., 2000). Ophiolitic assemblages are most prevalent in the North Qilian belt, where Middle Cambrian and Middle to Late Ordovician populations have been identified from paleontological evidence (Xia et al., 1996). The ophiolites have also been divided on the basis of metamorphic grade of associated blueschists, with the Middle to Late Ordovician and Middle Cambrian assemblages corresponding to the low- and high-grade blueschist belts situated in the north and south of the North Qilian belt, respectively (Wu et al., 1993; Tian and Wu, 1994). Serpentinites are associated with both ophiolite populations, and were sampled from the Ta-Den and Ayougou localities in the low-grade blueschist belt, and from the Baijing temple and Qing–Shui localities in the high-grade blueschist belt (Fig. 1).

At the Ta-Den locality, a 200 m thick sequence of serpentinites is associated with pillow-lavas, blueschist and slates/phyllites (Xu et al., 1994). Dating of the metasedimentary rock sequence by K–Ar, Ar–Ar and Rb–Sr methods has yielded ages of 409–412 Ma (Tian and Wu, 1994; Smith et al., 1997), with the volcanic sequence interpreted as a supra-subduction or back-arc basin sequence (Chung and Smith, 2000). In the Ayougou section, Paleozoic oceanic strata occur in fault contact with an earlier Proterozoic ocean basin assemblage, with both sequences containing serpentinites and having been interpreted to represent ocean ridge strata (Chen, 1996; Zuo et al., 2000). At the Baijing temple locality, serpentinites are associated with a sequence of arc volcanic rocks and mica-schists derived from arc and crustal sources (Tseng, 1998; Tseng and Yang, 2000). At the Qing–Shui locality, the volcanic sequence is subordinate to sediments and a 1.5 km thick sequence of serpentinite is associated with blueschist, slate and phyllite of continental and arc provenance (Wu et al., 1993; Tian and Wu, 1994; Smith et al., 1997). Dating of the metasedimentary rock sequence at the Qing–Shui locality has yielded K–Ar, Rb–Sr and Ar–Ar ages of 442–449 Ma which can be interpreted as marking the time of metamorphism on basin closure (Tian and Wu, 1994; Smith et al., 1997). Ophiolitic strata and related volcanic rocks, thought to be Cambrian to Ordovician in age, are also found in the Lha-Jyi terrane of the South/Central Qilian belt (BGMRQP, 1991). Samples were taken from Chiu Tarn locality of the Lha-Jyi terrane where serpentinites occur as series of knolls in a fault-bounded unit between exposures of basaltic and andesitic volcanic rocks. Volcanic rocks including boninitic compositions are also present within the serpentinite unit in the Lha-Jyi terrane and have been interpreted as an ocean floor-supra subduction zone sequence (Lin, 1997).

3. Analytical procedures

Samples were cut into thin slivers using a diamond-tipped saw, taking care to avoid any visible alteration or veining. Saw marks were then removed using silicon carbide paste, and

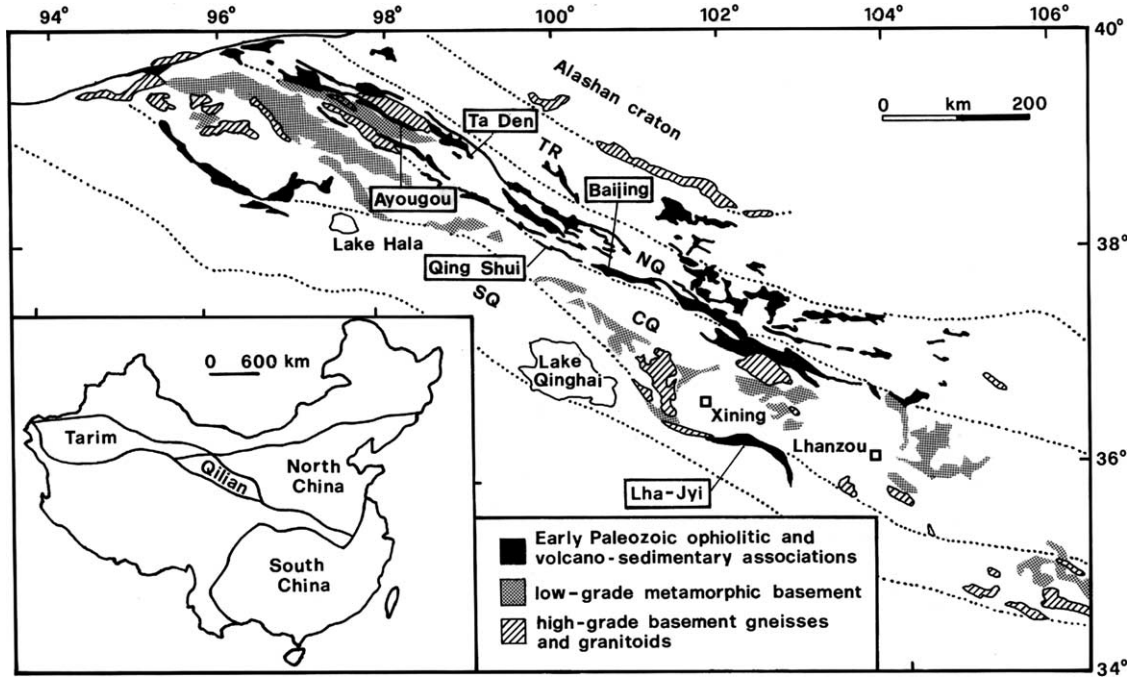

Fig. 1. Sampling locations relative to the principal tectonic divisions (TR, Transition Region; NQ, North Qilian belt; CQ, Central Qilian belt; SQ, South Qilian belt; Xiong and Coney, 1985) of the Qilian fold belt. Inset, location of the Qilian belt in relation to the principal tectonic blocks of China. The distribution and division of ophiolitic and basement strata follows maps by BGMRGP (1989), BGMRQP (1991) and Wan et al. (2000).

Table 1
Major and trace element compositions for serpentinites from the Qilian fold belt

Sample	810I	811E	812C	812K	812K1	1-1R	6-3	2-3	7-2B	809-4	809-6B	809-09	809-14	809-22
Locality	TD	QS	BJ	BJ	BJ	AYp	AYp	AYc	AYc	LJ	LJ	LJ	LJ	LJ
Protolith	LH	HZ	HZ	DN	LH	LH	LH	LH	OPX	DN	HZ	HZ	HZ	LH
SiO_2	37.10	42.07	40.84	36.77	41.82	40.11	37.00	41.96	39.38	39.86	31.77	39.27	39.24	39.16
TiO_2	0.058	0.005	0.020	0.050	0.060	0.024	0.026	0.044	0.008	0.027	0.008	0.039	0.025	0.062
Al_2O_3	1.61	0.63	1.21	1.03	2.97	1.37	1.43	1.63	0.37	0.57	1.13	0.81	0.97	1.95
ΣFeO	7.41	4.98	6.07	6.47	6.70	6.20	5.90	7.13	6.59	6.08	6.85	7.21	6.31	6.11
MnO	0.086	0.104	0.060	0.080	0.060	0.130	0.136	0.127	0.051	0.371	0.082	0.100	0.096	0.093
MgO	32.75	34.85	37.63	38.99	35.02	35.32	37.00	37.03	38.39	40.11	34.91	39.97	39.51	37.69
CaO	3.58	0.27	1.21	0.67	0.53	0.03	0.04	0.06	0.18	0.01	0.58	0.53	0.49	1.26
K_2O	0.02	0.01	0.01	0.01	0.01	0.01	0.01	0.01	0.01	0.03	0.01	0.02	0.03	0.01
Na_2O	0.01	0.08	0.02	0.05	0.06	0.01	0.09	0.01	0.08	0.04	0.01	0.04	0.08	0.09
P_2O_5	0.012	0.004	0.01	0.050	0.100	0.018	0.007	0.017	0.006	0.038	0.015	0.038	0.034	0.037
LOI	16.20	16.99	13.02	16.40	12.59	13.88	16.27	13.91	14.57	12.92	32.28	11.21	14.94	12.32
Total	98.836	99.993	100.10	100.57	99.920	97.102	97.909	101.93	99.635	100.06	107.64	99.237	101.72	98.782
Major elements normalised to 100 wt% on a volatile-free basis														
SiO_2	44.90	50.68	46.90	43.69	47.89	48.20	45.32	47.67	46.29	45.74	42.15	44.61	45.22	45.29
TiO_2	0.07	0.01	0.02	0.06	0.07	0.03	0.03	0.05	0.01	0.03	0.01	0.04	0.03	0.07
Al_2O_3	1.95	0.76	1.39	1.22	3.40	1.65	1.75	1.85	0.43	0.65	1.50	0.92	1.12	2.26
ΣFeO	8.97	6.00	6.97	7.69	7.67	7.45	7.23	8.10	7.75	6.98	9.09	8.19	7.27	7.07
MnO	0.10	0.13	0.07	0.10	0.07	0.16	0.17	0.14	0.06	0.43	0.11	0.11	0.11	0.11
MgO	39.63	41.99	43.21	46.32	40.10	42.44	45.32	42.07	45.13	46.03	46.32	45.41	45.53	43.59
CaO	4.33	0.32	1.39	0.80	0.61	0.04	0.05	0.07	0.21	0.01	0.77	0.60	0.56	1.46
K_2O	0.02	0.01	0.01	0.01	0.01	0.01	0.01	0.01	0.01	0.03	0.01	0.02	0.03	0.01
Na_2O	0.01	0.10	0.02	0.06	0.07	0.01	0.11	0.01	0.09	0.05	0.01	0.05	0.09	0.10
P_2O_5	0.01	0.01	0.01	0.06	0.11	0.02	0.01	0.02	0.01	0.04	0.02	0.04	0.04	0.04
Cr	2903	2170	3814	2551	3160	2601	2984	3002	4473	2522	3266	2285	2093	2557
Ni	2394	1891	2058	2434	2042	2309	2340	2502	2890	2348	2784	2224	2398	2543
Cu	23	27	4	5	10	18	0	36	0	1	10	4	26	10
Zn	58	58	48	32	54	60	55	65	49	34	37	38	40	44
V	46	26	45	–	93	48	43	43	–	–	26	30	–	40
Zr	10.0	7.0	15.4	–	29.5	7.0	1.0	7.0	–	–	8.0	5.5	–	11.5
Sc	11	9.9	9.4	–	11.9	10.0	10.8	11.1	–	–	5.0	8.8	–	12.6
Ba	22	0	1	–	5	2	4	1	–	–	8	3	–	3
Rb	0.3	0.2	0.2	–	0.2	0.20	0.1	0.3	–	–	0.07	0.30	–	0.20
Sr	43	2.0	71	–	3.0	1.0	5.0	2.0	–	–	13	3.0	–	4.0
Pb	0.39	0.0	0.27	–	0.75	0.13	0.33	0.10	–	–	0.38	0.00	–	1.34
Hf	0.08	0.02	0.01	–	0.13	0.03	0.03	0.04	–	–	0.02	0.02	–	0.08
Nb	0.14	0.07	0.26	–	0.75	0.06	0.15	0.07	–	–	0.18	0.06	–	0.10
Y	1.26	0.27	0.13	–	1.44	0.81	0.94	0.88	–	–	0.22	0.26	–	1.42
U	0.02	0.08	0.04	–	0.12	0.01	0.01	0.01	–	–	0.01	0.01	–	0.01
Th	0.02	0.04	0.03	–	0.24	0.03	0.01	0.03	–	–	0.05	0.05	–	0.06
La	0.20	0.10	0.10	–	0.29	0.06	0.03	0.05	–	–	0.13	0.15	–	0.23
Ce	0.32	0.16	0.19	–	0.61	0.13	0.12	0.11	–	–	0.21	0.26	–	0.41
Pr	0.06	0.03	0.02	–	0.08	0.02	0.02	0.02	–	–	0.03	0.03	–	0.06
Nd	0.25	0.10	0.09	–	0.34	0.11	0.14	0.08	–	–	0.10	0.13	–	0.26
Sm	0.10	0.02	0.02	–	0.14	0.04	0.06	0.04	–	–	0.02	0.02	–	0.09

(*continued on next page*)

Table 1 (*continued*)

Sample	810I	811E	812C	812K	812K1	1-1R	6-3	2-3	7-2B	809-4	809-6B	809-09	809-14	809-22
Locality	TD	QS	BJ	BJ	BJ	AYp	AYp	AYc	AYc	LJ	LJ	LJ	LJ	LJ
Protolith	LH	HZ	HZ	DN	LH	LH	LH	LH	OPX	DN	HZ	HZ	HZ	LH
Eu	0.05	0.01	0.01	–	0.03	0.02	0.02	0.02	–	–	0.01	0.01	–	0.04
Gd	0.15	0.04	0.02	–	0.25	0.08	0.08	0.09	–	–	0.04	0.03	–	0.14
Tb	0.03	0.01	0.00	–	0.04	0.02	0.02	0.02	–	–	0.01	0.01	–	0.03
Dy	0.22	0.05	0.02	–	0.25	0.13	0.14	0.15	–	–	0.04	0.03	–	0.22
Ho	0.05	0.01	0.00	–	0.06	0.03	0.03	0.03	–	–	0.01	0.01	–	0.05
Er	0.15	0.03	0.02	–	0.19	0.09	0.10	0.10	–	–	0.03	0.03	–	0.16
Yb	0.17	0.04	0.02	–	0.22	0.10	0.11	0.11	–	–	0.04	0.04	–	0.16
Lu	0.03	0.01	0.00	–	0.04	0.02	0.02	0.02	–	–	0.01	0.01	–	0.03
$(La/Yb)_n$	0.79	1.56	3.21	–	0.82	0.39	0.15	0.30	–	–	2.05	2.55	–	0.80
$(La/Sm)_n$	1.24	2.77	2.77	–	1.26	0.91	0.30	0.78	–	–	4.02	3.92	–	1.61
Eu/Eu*	1.27	1.08	1.50	–	1.98	1.08	0.92	1.06	–	–	1.11	1.30	–	1.08

Localities: AY, Ayougou (p, Proterozoic, c, Caledonian); BJ, Baijing temple; LJ, Lha-Jyi; QS, Qing–Shui, TD, Ta-Den. Protoliths as identified from petrography and rare earth element profiles: LH, lherzolite; HZ, harzburgite; DN, dunite; OPX, orthopyroxenite.

slivers reduced to a coarse grain-size using a stainless steel pestle and mortar. Aliquots were further ground using a tungsten carbide ball mill and analysed by XRF at Cheng Kung University or by XRF/ICPMS at the Geoanalytical Laboratory, Washington State University. For isotopic analysis, Sm and Nd were extracted from approximately 1 g of sample chips using Eichrom extraction chromatographic materials REE-resin and LN-resin following conventional sample dissolution in HF/HNO_3 (Smith and Huang, 1997). Blanks ranged from 270 to 315 pg Nd with the background $^{143}Nd/^{144}Nd$ ratio estimated at 0.512400. Sample/background ratios were between 200 and 6000 and were generally greater than 700, such that contributions from the blank would lie within the range of analytical uncertainty, hence background corrections have not been applied. Isotopic measurements were performed on a MAT262 thermal ionisation mass spectrometer at Cheng Kung University. $^{143}Nd/^{144}Nd$ ratios were normalised to $^{146}Nd/^{144}Nd = 0.7219$ and are reported relative to 0.511855 for the La Jolla standard, with age corrections being made assuming present day $^{143}Nd/^{144}Nd = 0.512638$ and $^{147}Sm/^{144}Nd = 0.1967$ for CHUR.

4. Results

4.1. Mineralogy

The serpentinites are dark grey or dark green and are massive or foliated. Their mineralogy consists of serpentine minerals, original igneous olivine, pyroxenes, Cr–spinel, magnetite–hematite–goethite, and carbonate. The serpentine minerals commonly show mesh- and lattice type textures, occasionally enclosing original olivine. From the abundances of olivines and pyroxenes, the protoliths of the serpentinites at the Baijing temple, Qing–Shui and Lha-Jyi localities include lherzolite (samples 809-22, 812K1), harzburgite (809-9, 809-14, 811E) and dunite (809-4, 812K), whereas samples from the Ta-Den and Ayougou localities have lherzolitic (810I, 1-1R, 6-3, 2-3) or orthopyroxenitic (7-2) protoliths. Strong carbonitisation (magnesite and dolomite) and silicification in samples 812C from the Baijing temple locality and 809-6B from the Lha-Jyi terrane locality precluded petrographic identification of original rock types.

4.2. Major and trace element composition

Major and trace element compositions for representative samples are presented on Table 1. Unfortunately, for severely altered samples, normalisation to 100% results in errors if the composition of even one major element has changed (Prinzhofer and Allègre, 1985). In the Qilian sample suite, loss on ignition ranges from 11 to 17 wt% for most samples, and over 32 wt% in sample 809-6B which is severely altered. Nonetheless, major element contents are broadly consistent with the mineralogical classification, with MgO contents ranging from 39.6 wt% in the lherzolitic samples to 46.3 wt% in dunitic compositions when recalculated on a volatile-free basis. Less altered oceanic peridotite suites, such

as from the Papuan ultramafic belt (loss on ignition less than 3.3 wt%; Jacques and Chappell, 1980) and the Ligurides (loss on ignition 2–4 wt%; Rampone et al., 1996), follow melting trends of decreasing SiO_2, Al_2O_3 and CaO with increasing MgO (Fig. 2). Such suites show similar major element correlations to xenolith suites representing young continental mantle beneath accreted terranes, which have not undergone alteration (e.g. Xue et al., 1990; Zangana et al., 1999), and define trends which pass through the average upper mantle composition of McDonough (1990). The Qilian samples define steeper SiO_2–MgO trends and have flat arrays in Al_2O_3–MgO and CaO–MgO space (Fig. 2) are thus more similar to serpentinised oceanic peridotite suites such as from the Halmahera ophiolite (Ballantyne, 1992) and Leg 153 peridotites from the Mid Atlantic Ridge (Brandon et al., 2000) which have suffered more severe alteration. The variation thus follows trends of decreasing MgO, CaO and Al_2O_3, increasing SiO_2 demonstrated in experimental serpentinisation studies (Janecky and Seyfried, 1986).

To avoid problems resulting from normalisation of major element compositions, studies of serpentinites have focused on trace element features such as rare earth element (REE) profiles (e.g. Sharma and Wasserburg, 1996; Gruau et al., 1998). Harzburgitic samples from the Lha-Jyi and Qing–Shui localities have U-shaped REE patterns ($(La/Yb)_n = 1.5–3.2$, $(La/Sm)_n = 2.7–4.0$) with low middle rare earth element (MREE) abundances. In contrast, lherzolitic samples 809-22 from the Lha-Jyi locality, 812K1 from Baijing temple, and those from the Ayougou and Ta-Den localities have higher total REE contents and show progressive MREE–LREE depletion or moderate MREE depletion with slight LREE enrichment ($(La/Yb)_n = 0.1–0.8$, $(La/Sm)_n = 0.3–1.6$). Correspondingly, the U-shaped profiles and strong MREE depletion seen in the profiles for the heavily altered samples 809-6B and 812C suggests the protoliths of these samples were harzburgites. The majority of Qilian samples have positive or no Eu anomalies, except for 812K1, which has a negative anomaly. In HREE–MREE patterns, lherzolitic samples are similar to peridotites representing residues from melting at ocean ridge environments, whereas harzburgitic samples are more similar to highly depleted peridotites from supra-subduction zone environments (Fig. 3). However, a common feature of all samples is greater LREE enrichment than typically seen in other oceanic peridotite suites. Trace element profiles are characterised by abundances of moderately compatible and compatible elements (HREE, Y, V, Sc, Zn, Ni, Cr) similar to in oceanic peridotites following trends expected for variable degrees of melt extraction (Fig. 4). However, incompatible trace elements including LREE, high field strength elements (HFSE) and large ion lithophile elements (LILE) are enriched, with the degree of enrichment broadly increasing with incompatibility of the element. Positive spikes are also observed in the profiles at Sr, U and to a lesser extent Ba. The enrichments in HFSE illustrated by Nb and Hf in Fig. 4 are also noted for Ti and Zr (Table 1), although as these elements are analysed by XRF, they are considered less reliable at the abundance levels present in the samples.

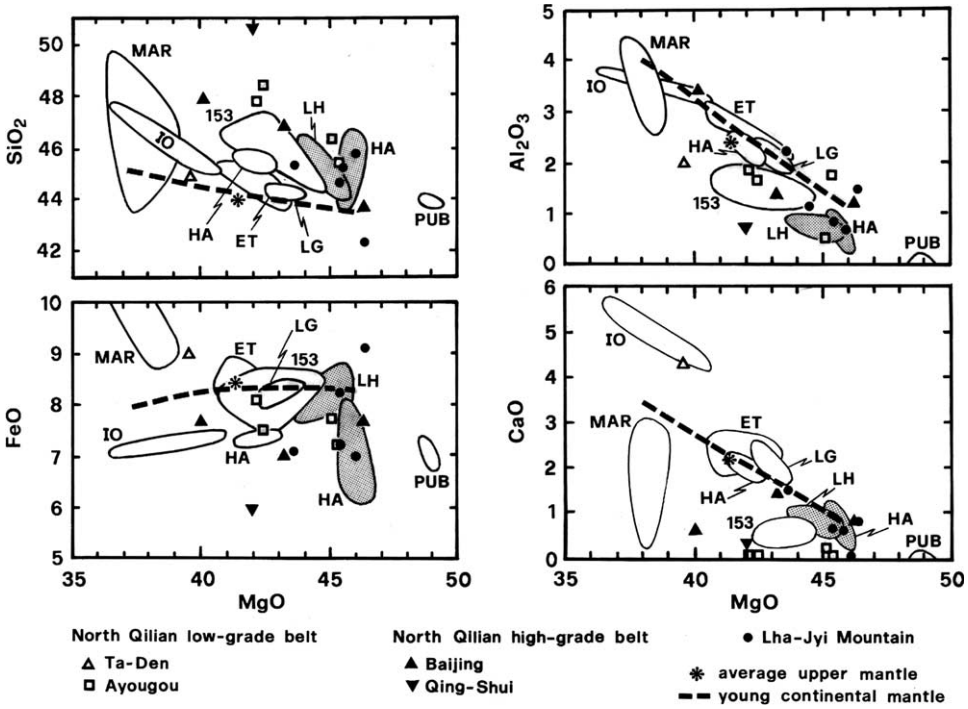

Fig. 2. Variation of major element composition with MgO in Qilian serpentinites compared to peridotites from ocean floor (ET, Erro-Tobio; Scambelluri et al., 2001; IO, Indian Ocean; Hekinian, 1982; LG, Ligurides; Rampone et al., 1996; MAR, Mid Atlantic Ridge; Hekinian, 1982; Leg 153, Brandon et al., 2000; PUB, Papuan ultramafic belt; Jacques and Chappell, 1980) and fore-arc settings (shaded; HA, Halmahera ophiolite; Ballantyne, 1992; LH, Lihir; McInnes et al., 2001). Also shown are compositions for average upper mantle (McDonough, 1990) and trends defined by mantle xenoliths representing young continental mantle beneath accreted terranes (Xue et al., 1990).

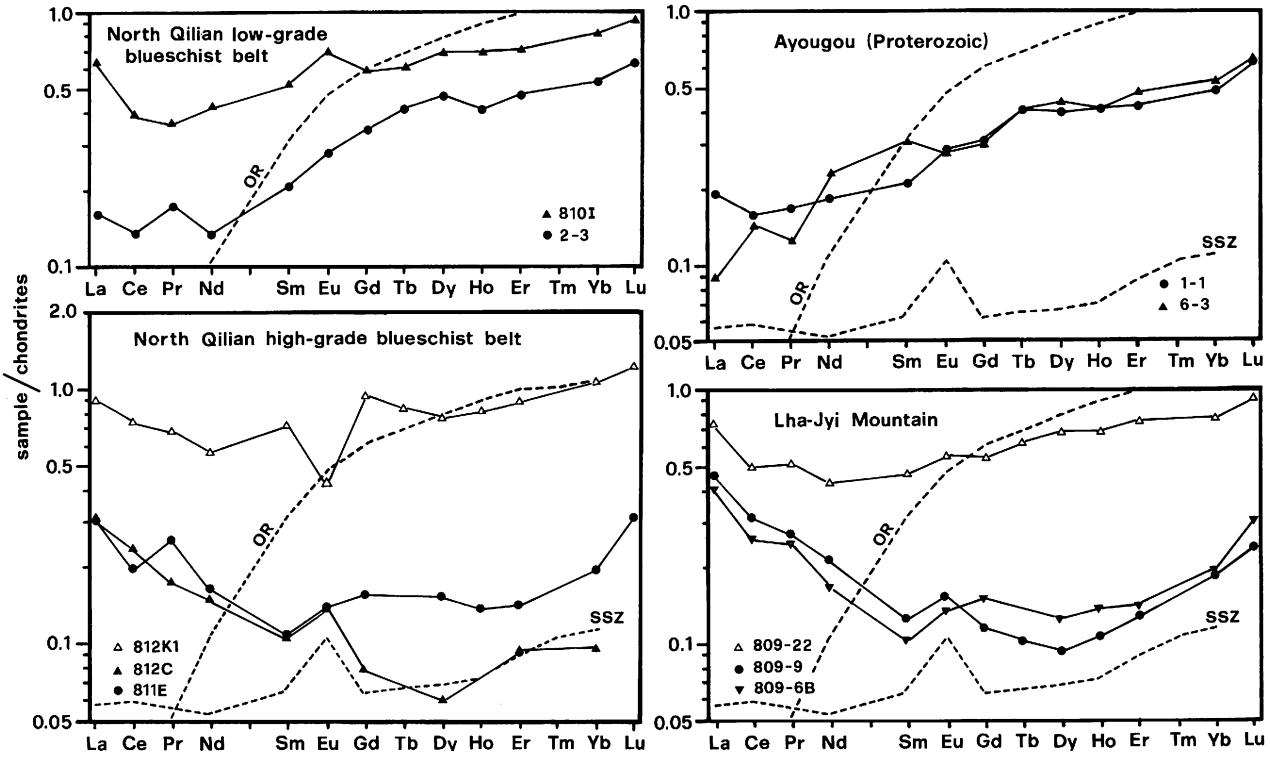

Fig. 3. Chondrite-normalised rare earth element profiles for Qilian serpentinites. Also shown are patterns for lherzolite and harzburgite compositions formed at ocean ridge (OR) and supra-subduction zone settings (SSZ), respectively (after Rampone et al., 1996; Franz et al., 2002). Normalising abundances are from Taylor and Gorton (1977).

4.3. Isotopic composition

Previous studies (e.g. Sharma and Wasserburg, 1996; Gruau et al., 1998) have noted extreme internal isotopic inhomogeneity in serpentinite samples, resulting in different aliquots varying by up to $4\varepsilon_{Nd}$ units on age correction for Early Paleozoic samples. Discrepancies in element abundances analysed by mass spectrometry isotope dilution and ICPMS were also noted by Sharma and Wasserburg (1996). However, for the samples analysed in this study, good agreement was noted between the analytical methods in most cases (Tables 1 and 2). Replicate analyses of sample 810I from the Ta-Den locality yielded $\varepsilon_{Nd}(T)$ values within the range of analytical uncertainty. A range of $\varepsilon_{Nd}(T)$ of 1.8 units was noted for aliquots of 809-22 from the Lha-Jyi locality and up to three epsilon units for samples from the Ayougou Proterozoic section (Table 2), which may in part reflect uncertainties in the age to which the samples were corrected. However, an advantage of sample heterogeneity is that it facilitates the construction of internal isochrons, and serpentinites in other ocean basins have sometimes retained Sm–Nd age information (e.g. Sharma et al., 1995). Correlations between $^{147}Sm/^{144}Nd$ and $^{143}Nd/^{144}Nd$ are seen in the Qilian samples for all but the Baijing and Qing–Shui suites where the number of samples is limited (Fig. 5). The best correlation is observed for the Ayougou samples previously mapped as belonging to the Paleozoic suite, where a large range in $^{147}Sm/^{144}Nd$ in lherzolitic and pyroxenitic samples gives a slope corresponding to an Early Silurian age of 422 ± 20 Ma with initial $\varepsilon_{Nd}(T) = +6.8$ (Fig. 5), similar to peridotites from the Ballantrae ophiolite (Thirlwall and Bluck, 1984) of southwest Scotland (Fig. 6). Samples from Ayougou mapped as part of the Proterozoic assemblage (Chen, 1996) lie along a line corresponding to an apparent age of 1033 Ma with $\varepsilon_{Nd}(T) = -2.9$, which lies within the age ranges reported for amphibolites (1040–1071 Ma, Rb–Sr and K–Ar methods; BGMRGP, 1989), granitoids (1060 ± 39 Ma, Sm–Nd; Smith et al., 2000) and gneisses (930 ± 30 Ma, U–Pb, Wan et al., 2000; 987 ± 29 Ma, Rb–Sr, Smith et al., 2000) from the Central and South Qilian belts. However, the ε_{Nd} value is low for mantle derived rocks (Fig. 6), and the correlation is too dependent on a single sample with considerable scatter observed at high $^{147}Sm/^{144}Nd$ and $^{143}Nd/^{144}Nd$ for the age to be treated with confidence.

Sample 810I from the Ta-Den locality lies close to the isochron for the Paleozoic Ayougou samples. If the age for the Ayougou serpentinites is taken as representative for the northern low-grade blueschist belt of the North Qilian terrane, a comparable age for the Ta-Den serpentinites yields $\varepsilon_{Nd}(422\text{ Ma}) = +5.6$, lower than for the associated MORB-like basaltic rocks which have $\varepsilon_{Nd}(422\text{ Ma}) = +7.3$ to $+8.2$ (Fig. 6). As no age information can be extracted from the Baijing and Qing–Shui samples, the isotopic compositions for these localities have been corrected to an assumed age of 450 Ma, slightly older than the timing of basin closure, on account of evidence in the following section for exchange of incompatible elements with the sedimentary pile. The resulting ε_{Nd} values for the Qing–Shui and Baijing serpentinites are low ($\varepsilon_{Nd}(450\text{ Ma}) = +2.3$ to -3.8), but overlap those of the associated volcanic rocks

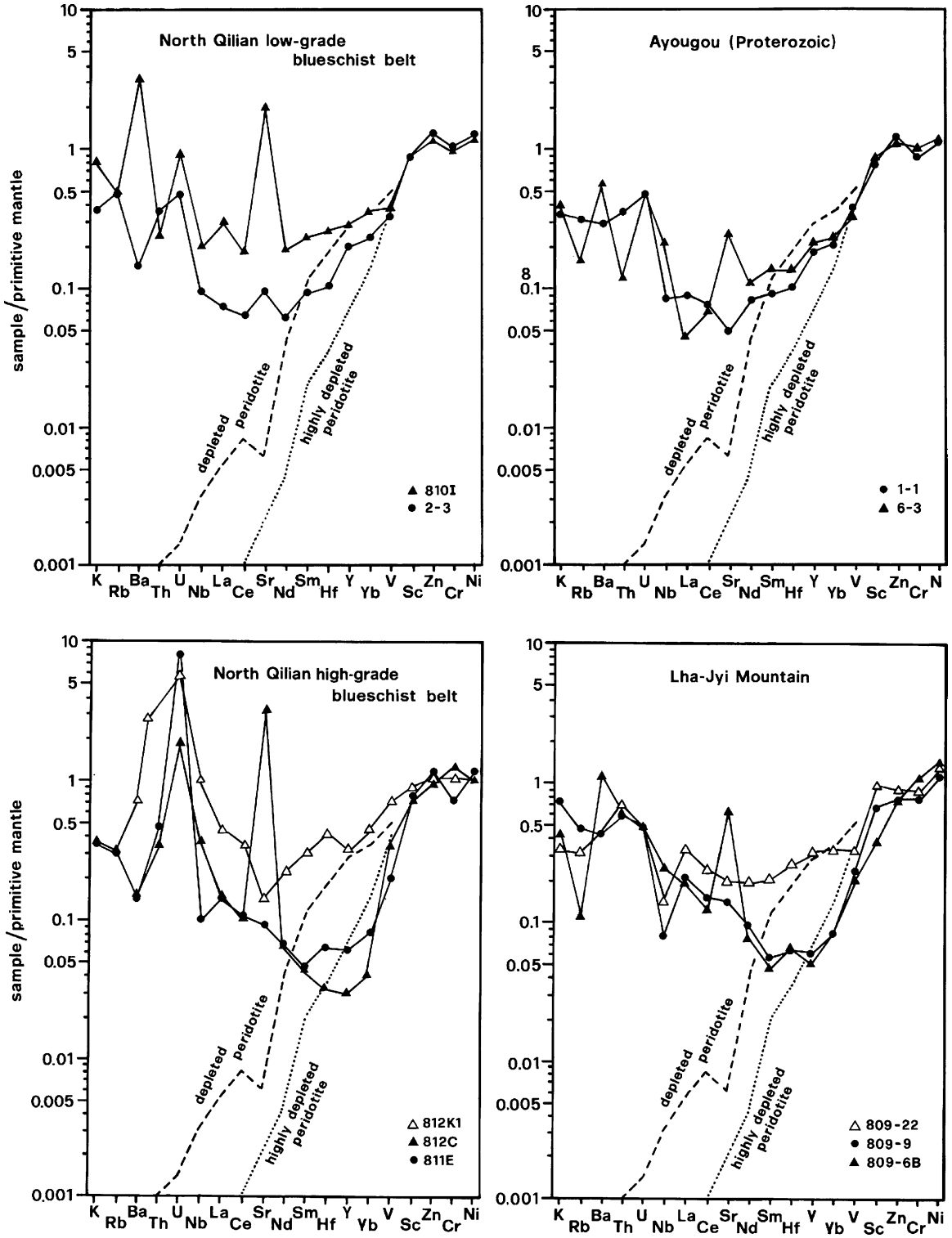

Fig. 4. Primitive mantle-normalised trace element variation diagram for Qilian serpentinites relative to profiles for depleted peridotites (average of compositions from Liguride peridotites from Rampone et al., 1996) and highly depleted peridotites (average for Urals harzburgites from Sharma and Wasserburg, 1996). Elements are arranged in order of increasing incompatibility from right to left. Normalising abundances for elements from K to Yb are from Sun and McDonough (1989), values for V to Ni are from Taylor and McLennan (1985).

(ε_{Nd}(450 Ma) = +1 to +4) and are similar to those of the Thetford Mines peridotites (ε_{Nd}(490 Ma) = +4.2 to −1.4; Shaw and Wasserburg, 1984) in the Appalachian belt (Fig. 6). In the Lha-Jyi suite, aliquots of lherzolite 809-22 define a linear correlation but the range of isotopic variation is small. The majority of arc volcanic rocks (Lin, 1997) and harzburgites from this locality also lie along the same line, yielding an apparent age of 670 Ma (Fig. 5). However, other samples lie close to a reference line whose slope would correspond to an age of 450 Ma. The isotopic data have thus been corrected to an

Table 2
Whole rock serpentinite Sm–Nd isotopic compositions

Sample	Locality	Sm (ppb)	Nd (ppb)	$^{147}Sm/^{144}Nd$	$^{143}Nd/^{144}Nd$	$\varepsilon_{Nd}(T)$
North Qilian, low-grade blueschist belt (T=422 Ma)						
810I (i)	TD	116.9	302.0	0.2342	0.513033±26	+5.7
810I (ii)	TD	124.5	340.0	0.2215	0.512987±08	+5.5
2-3	AY	51.10	85.73	0.3606	0.513426±36	+6.5
6-4	AY	20.99	256.3	0.0495	0.512585±07	+6.9
7-2A	AY	17.63	105.6	0.1010	0.512663±08	+5.7
7-2B	AY	30.08	273.8	0.0665	0.512599±15	+6.3
7-2C	AY	17.09	24.99	0.4137	0.513557±31	+6.2
North Qilian, high-grade blueschist belt (T=450 Ma)						
811E	QS	34.66	105.0	0.1997	0.512463±24	−1.0
812K1	BJ	134.4	365.9	0.2222	0.512596±12	−2.3
812C	BJ	21.79	95.60	0.1379	0.512660±14	+3.8
North Qilian belt, Proterozoic (T=1033 Ma)						
1-1						
(i)	AY	47.28	117.6	0.2432	0.512747±15	−4.0
(ii)		65.11	321.6	0.1225	0.512039±15	−1.9
4-2						
(i)	AY	95.30	234.0	0.2464	0.512939±60	−0.7
(ii)		76.28	193.9	0.2380	0.512986±16	+1.3
6-3						
(i)	AY	91.26	201.1	0.2745	0.513009±15	−3.1
(ii)		56.58	137.4	0.2491	0.512987±09	−0.1
Lha-Jyi terrane (T=500 Ma)						
809-G	LJ	5.791	25.54	0.1372	0.512405±19	−0.7
809-H	LJ	20.42	70.43	0.1754	0.512456±08	−2.2
809-3	LJ	4.375	17.90	0.1479	0.512564±58	+1.7
809-4	LJ	225.7	812.0	0.1681	0.512554±12	+0.2
809-5	LJ	44.42	146.1	0.1840	0.512636±16	+0.8
809-6B	LJ	20.03	80.01	0.1514	0.512423±10	−1.3
809-8A	LJ	69.45	313.7	0.1339	0.512427±32	−0.1
809-8B	LJ	11.70	46.18	0.1533	0.512498±14	0.0
809-9	LJ	42.13	141.5	0.1801	0.512636±16	+1.0
809-21B	LJ	4.309	17.05	0.1529	0.512484±24	−0.2
809-22						
(i)	LJ	78.20	197.4	0.2397	0.512866±85	+1.7
(ii)		105.2	212.2	0.2999	0.513154±06	+3.5
(iii)		93.49	228.8	0.2472	0.512943±94	+2.7
809-23	LJ	59.98	126.8	0.2862	0.512842±10	−1.7

Localities: AY, Ayougou; BJ, Baijing temple; LJ, Lha-Jyi; QS, Qing–Shui; TD, Ta-Den. Ages from Fig. 5, except for North Qilian high-grade blueschist belt and Lha-Jhyi terrane where ages are assumed. Replicate analyses of whole rock chips to test sample heterogeneity are indicated as (i)–(iii).

assumed stratigraphic age of 500 Ma in Table 2. The resulting ε_{Nd} values overlap those of the volcanic rocks and are comparable to the $\varepsilon_{Nd}(T)$ values of the Thetford Mines peridotites and serpentinites in the high-grade blueschist belt of the North Qilian terrane.

5. Discussion

Trace element and isotopic variations in serpentintes have previously been attributed to a range of processes including partial melting, melt metasomatism, and introduction of a crustal component by hydrothermal alteration or groundwater interaction. Partial melting in the ocean ridge environment would be expected to produce systematic decreases in incompatible trace element content as observed in depleted mantle peridotites (Prinzhofer and Allègre, 1985; Gruau et al., 1998). The mechanism is therefore inadequate to explain the U-shaped REE profiles in Figs. 3 and 4, nor can it explain departures from depleted mantle isotopic compositions in the Qilian samples. The melt metasomatism model envisages infiltration of residual peridotites by later stage melts in the ocean ridge environment. The effect on major element composition is to refertilise the peridotite compositions along the melting trend (Elthon, 1992), while isotopic compositions would not change significantly unless there was a long hiatus between the melting and metasomatic events (Sharma and Wasserburg, 1996). The mechanism might potentially account for elevated Nb, Th and LREE in the Paleozoic Ayougou serpentinites on account of their MORB-like $\varepsilon_{Nd}(T)$ values, but would not explain the departure of the major element compositions of these samples from the mantle melting trends, nor explain the isotope systematics of samples from the other localities where $\varepsilon_{Nd}(T)$ values are significantly lower than for Caledonian- or older mantle-derived rocks. Groundwater interaction would be expected to preferentially modify the more mobile elements such as the alkalis, alkaline earths and

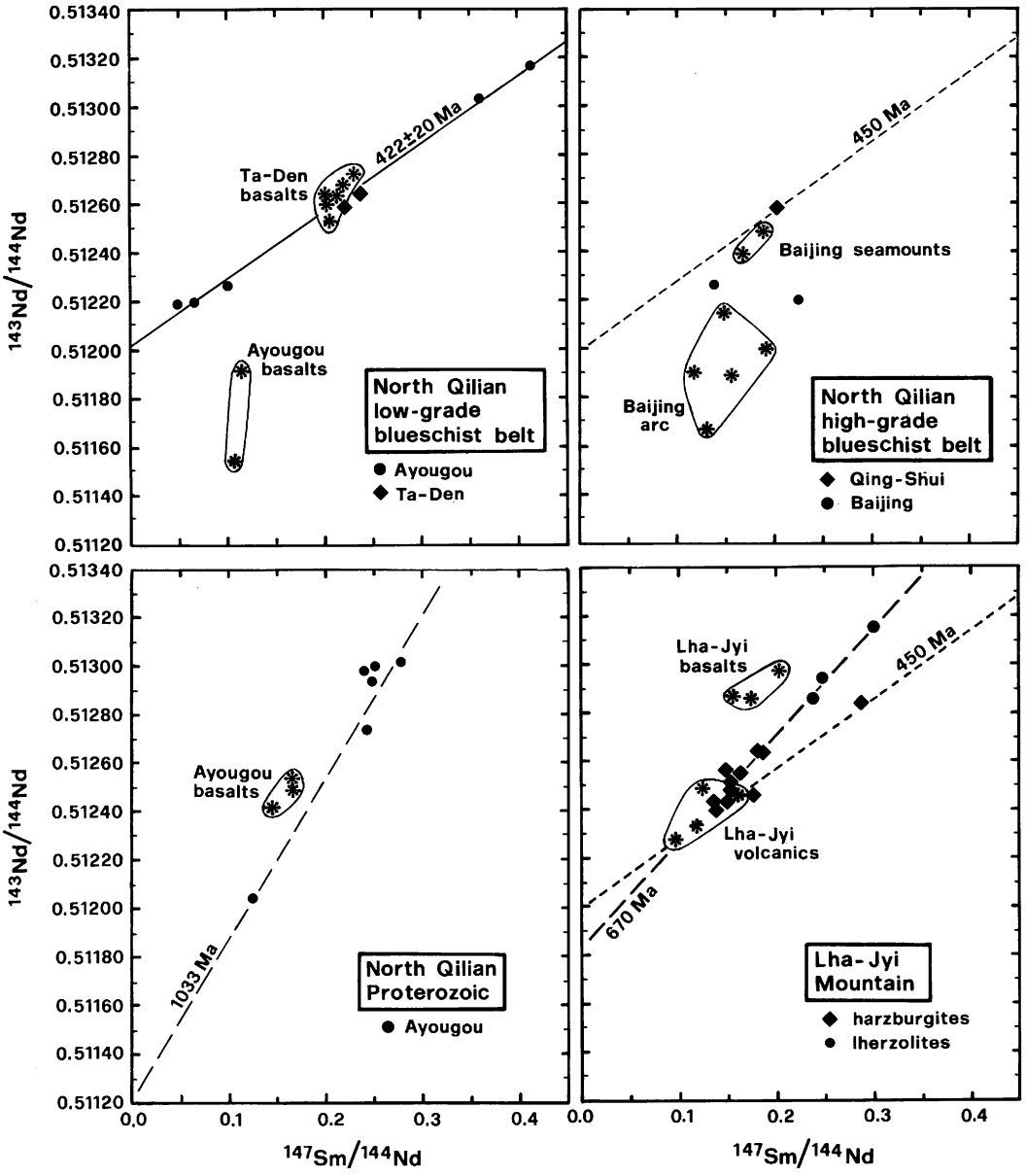

Fig. 5. Variation of $^{147}Sm/^{144}Nd$ with $^{143}Nd/^{144}Nd$ in Qilian serpentinites. Data for associated volcanic rocks is also shown: Lha-Jyi (Lin, 1997); Ayougou (Chen, 1996), Ta-Den (Chung and Smith, 2000), Baijing temple (Tseng, 1998).

U, although mobilisation of REE was also proposed by Gruau et al. (1998). Such a process could potentially explain the spikes at Sr, U and Ba in the trace element profiles of samples 809-6B, 812C, 810I and 6-3 from the mobility of these elements in near-surface environments. However, it is considered unlikely that the mechanism would produce enrichments in immobile elements such as the HFSE and Th, and is therefore discounted as the principal control on Qilian serpentinite composition.

The susceptibility of peridotites to hydrothermal alteration has been suggested to be related to composition, with harzburgites being more susceptible than lherzolites on account of the resistance of diopside to alteration, as this mineral contains much of the trace element budget (Menzies et al., 1993). The results of such alteration are also dependent on fluid composition. Interaction with pure seawater has been suggested to have little effect on Sm–Nd isotope systematics on account of the low Nd content of seawater (Menzies et al., 1993). However, studies of altered MORB have indicated both the trace element content and Nd isotopic composition of hydrothermal fluids to be modified by interaction with sediments, particularly in proximity to a continental margin where the sediment pile is thickest (Verma, 1992; Jochum and Verma, 1996). Under such conditions, incompatible elements traditionally regarded as immobile such as the HFSE and Th, may become enriched in altered MORB, likely as the result of mobilisation in Cl-rich brines. Similarly, $^{87}Sr/^{86}Sr$ ratios higher than for seawater have been observed in serpentinites due to the interaction of hydrothermal fluids with the sediment pile (Snow et al., 1993; O'Hanley, 1996). Such alteration may be modelled

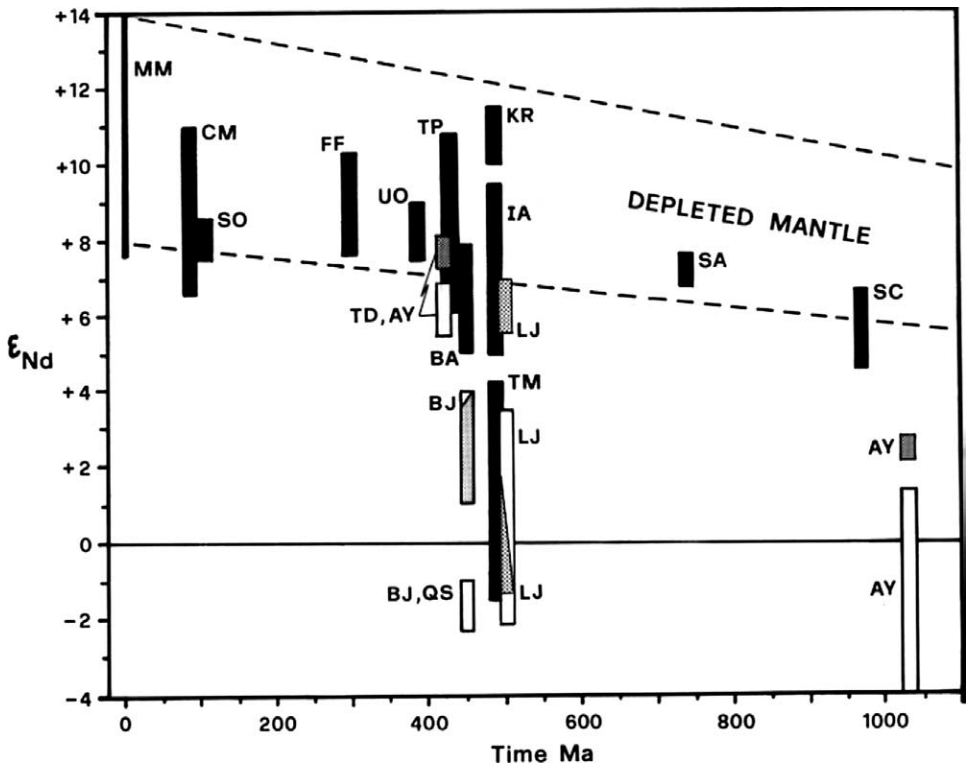

Fig. 6. Variation in ε_{Nd} of Qilian serpentinites (unshaded; AY, Ayougou; BJ, Baijing temple; LJ, Lha-Jyi; QS, Qing-Shui; TD, Ta-Den localities) and associated volcanic rocks (grey: Chen, 1996; Lin, 1997; Tseng, 1998) relative to Neoproterozoic-Phanerozoic oceanic assemblages (black). Abbreviations: BA, Ballantrae ophiolite (Thirlwall and Bluck, 1984); CM, Cretaceous MORB (Jahn et al., 1980); FF, Fennell Formation (Smith and Lambert, 1995); KR, Kings River ophiolite (Shaw et al., 1987); IA, Iapetus ophiolites (Jacobsen and Wasserburg, 1979; Smith et al., 1990); MM, Modern MORB (Ito et al., 1987); SA, Saudi Arabian ophiolites (Claesson et al., 1984); SC, South China ophiolites (Li et al., 1997); SO, Semail ophiolite (McCulloch et al., 1981); UO, Urals ophiolite (Edwards and Wasserburg, 1985); TD Ta-Den ophiolite (Chung and Smith, 2000), TM Thetford Mines igneous complex (Shaw and Wasserburg, 1984); TP Trinity peridotite (Jacobsen et al., 1984).

by dividing element concentrations by those of the unaltered sample to yield enrichment factors (Fig. 7). For the Qilian serpentinites, original compositions were estimated by assuming the lherzolitic samples had a trace element profile similar to depleted peridotites from the Ligurides reported by Rampone et al. (1996), which they resemble in moderately compatible and compatible element (V to Ni; Fig. 4) content. Correspondingly, compositions of the harzburgitic samples were compared to the highly depleted peridotites in Sharma and Wasserburg (1996), with concentrations for elements not reported by these authors estimated by extrapolation. The resulting enrichment patters for Qilian lherzolitic compositions show considerable similarities with the patterns for altered MORB, notably in the stepwise profile of the patterns despite enrichment factors being considerably greater. The lherzolitic samples thus show only slight enrichment in Y, HREE, Hf, Sm and Nd (enrichment factors (5), moderate enrichment in Sr, Ce, La, Nb (enrichment factors 5–500), and strong enrichments in alkalis, alkaline earths, Th and U (enrichment factors 200–10,000) (Fig. 7a and b). Profiles for the harzburgitic samples (Fig. 7c) differ from lherzolitic compositions in one key aspect, notably the break in pattern between low and moderate enrichment factors occurs between Sm and Nd in harzburgitic samples as compared to between Nd and Sr in the lherzolitic compositions. Thus in the harzburgitic samples, Y, HREE, Hf and Sm have enrichment factors of less than 5, whereas Nd, Sr, Ce, La, Nb have enrichment factors of 5–500. Potassium, Rb, Ba, Th, U also behave as a group, but with greater enrichment factors (3000–100,000) compared to in the lherzolitic samples (Fig. 8).

The suitability of hydrothermal alteration for explaining the trace element enrichments is supported by similarities between the harzburgite patterns and those of sediments from the Qilian belt normalised to unaltered peridotite compositions (Fig. 7). The mechanism may also explain the low ε_{Nd} values of some of the serpentinites, as although changes to Nd isotopic composition during the alteration of MORB are generally of the order of 0.5 epsilon units (Verma, 1992), the enrichment in Nd in harzburgitic samples is up to 15 times greater (Fig. 7). Alteration would therefore be expected to cause the isotopic composition of such samples to be strongly influenced by Nd derived from the sediment assemblages, which in the high-grade blueschist belt of the North Qilian belt have $\varepsilon_{Nd}(450\ Ma) = +1$ to -8 (Smith et al., 1997). However, although harzburgites are found along ridge systems (e.g. Cannat et al., 1992; Lagabrielle et al., 1998), the plausibility of producing large percentages of very refractory residues by melting in ocean ridge environments has been questioned as the principal residue from MORB generation is expected to be a clinopyroxene-poor lherzolite

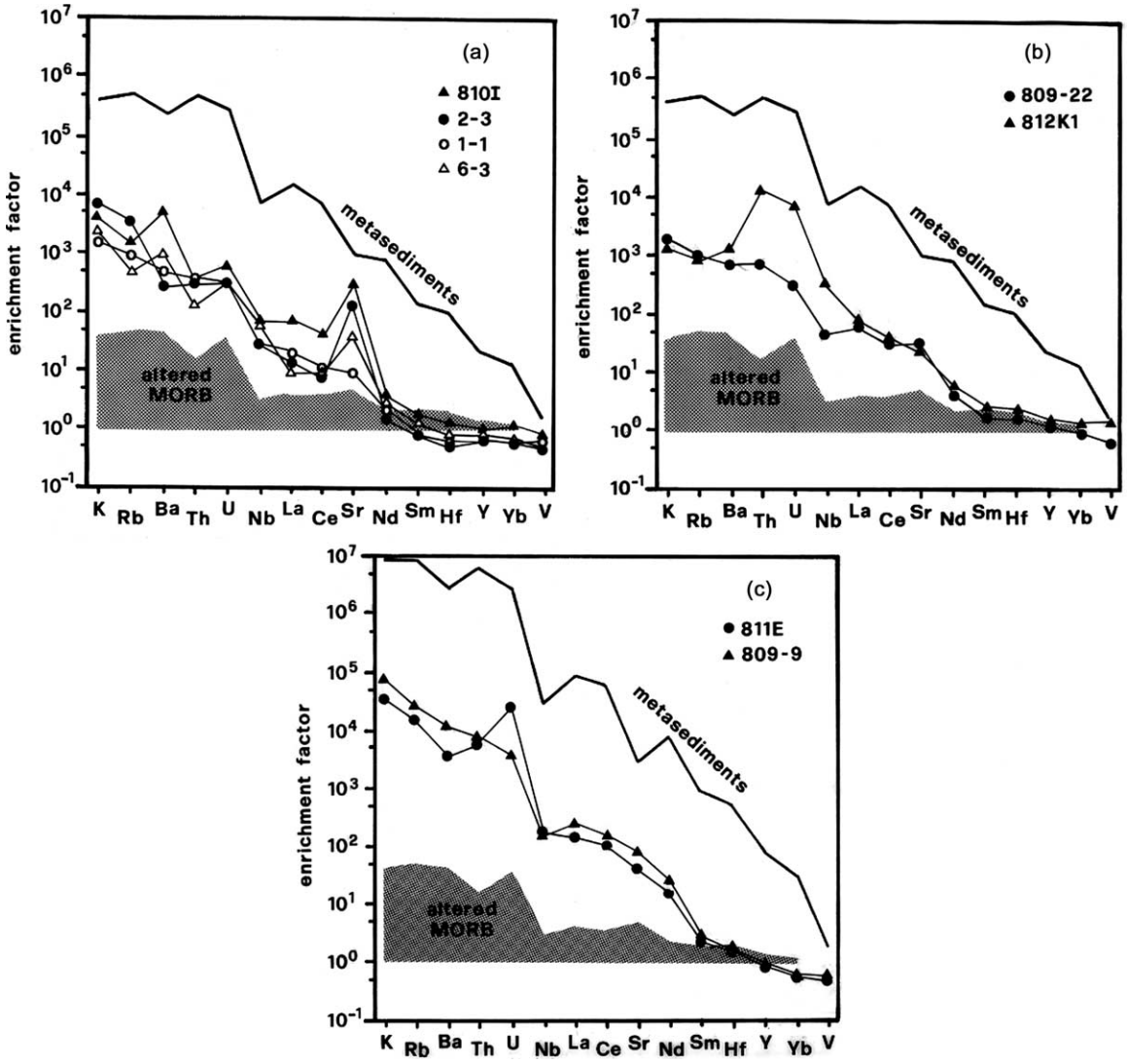

Fig. 7. Trace element enrichment factors for serpentinites of (a and b) lherzolitic composition (c) harzburgitic composition in the Qilian belt. Lherzolitic and harzburgitic compositions are normalised to depleted and highly depleted peridotite compositions in Fig. 4, respectively. Also shown are profiles for average sediment from the Qing–Shui locality (Smith et al., 1997) normalised to the respective peridotite composition, and altered MORB normalised to unaltered MORB compositions as described in Jochum and Verma (1996).

(e.g. Johnson and Fryer, 1990; Rampone et al., 1996). An alternative model is that features such as the strong MREE-depletion of many harzburgitic compositions reflects a second stage of melting as a result of fluxing fluids into the mantle (Franz et al., 2002). Such conditions may occur in a supra-subduction zone environment where in the model of Pearce et al. (1984), the pre-arc stage during the initial stages of subduction would be marked by fluids from the slab invading the oceanic lithosphere inducing the formation of boninitic melts. As the subduction zone evolves to the arc-stage, fluids are introduced to greater depths inducing melting of the asthenospheric part of the mantle wedge. Harzburgitic residues formed during the pre-arc stage would then lie in the fore-arc region where they would be subject to serpentinisation by fluids driven off the slab at low temperature. In such a scenario, enrichments in incompatible elements and isotopic composition could be inherited from the subducting slab. The presence of boninitic compositions within the serpentinite sequence in the Lha-Jyi section, in conjunction with the association of MORB-like basalts and arc volcanic rocks at this locality, suggests the sequence may represent such an assemblage. The interpretation is supported by the presence of weakly developed Nb anomalies in trace element profile (Fig. 4), and by compositional variation in chromian spinels from this locality (Lin, 1997) which overlaps that of both ocean ridge and arc peridotite assemblages as outlined by Dick and Bullen (1984). Likewise, the presence of harzburgitic compositions with similar compositional features to the Lha-Jyi samples in the Qing–Shui and Baijing localities is consistent with the supra-subduction setting inferred (Tseng, 1998; Tseng and Yang, 2000) for volcanic rocks in the high-grade blueschist belt of the North Qilian terrane.

The enrichment mechanisms identified above have important implications for the reliability of age information which may be extracted from the samples. The age for the Paleozoic Ayougou suite is realistic compared to ages for closure of the

basin, and can be interpreted to indicate that ocean ridge activity occurred some 10 million years before closure of the basin. The reliability of the age is supported by sample 2–3 from this suite being the only sample that does not deviate from the depleted peridotite trend before Sr in the trace element profiles in Fig. 4. In contrast, the Proterozoic Ayougou serpentinites have more refractory compositions than their Paleozoic counterparts as shown by their lower REE abundances in Fig. 3. The trace element profiles for the Proterozoic samples deviate from highly depleted peridotite compositions in elements more incompatible than Y in Fig. 4, with the implication that the Sm–Nd isotopic system has been disturbed and the correlation defined by this suite in Fig. 5 is the result of mixing between crustal and mantle components. Harzburgite and lherzolite samples from the Lha-Jyi terrane also deviate from the peridotite trace element profiles in elements more incompatible than Hf, suggesting the Sm–Nd isotope system has also been disturbed and that the apparent age of 670 Ma has no real significance

6. Conclusions

Isotopic and compositional variations in serpentinites from the Qilian fold belt are likely the result of multi-stage histories involving melt depletion and enrichments by aqueous fluids in ocean ridge and/or supra-subduction zone environments. Lherzolitic and harzburgitic compositions have both undergone enrichment in incompatible trace elements, with original Sm–Nd isotope systematics preserved only in Paleozoic samples from the Ayougou locality. The enrichment patterns suggest the fluids during serpentinisation of lherzolitic compositions were not pure seawater, but had been extensively modified by exchange of incompatible elements with the sediment veneer of the oceanic crust. The trace element and isotopic variations in the harzburgitic samples are consistent with the compositions representing more highly refractory residues that were altered in a similar fashion to the lherzolites. However, their compositions are also consistent with oceanic lithosphere that had undergone a second phase of melting in a supra-subduction zone environment, prior to serpentinisation in a fore-arc setting. The association of the harzburgitic samples with arc volcanic rocks suggests the latter of these alternatives is the more plausible. A further phase of alteration which imparted elevated contents of mobile elements such as U, Sr and Ba can be attributed to interaction with groundwater after obduction of the ophiolite sequence.

Acknowledgements

L.-Y. Huang is thanked for preparing samples for isotopic analysis. U. Knittel and C.-Y. Lan are thanked for reviews.

References

Ballantyne, P., 1992. Petrology and geochemistry of the plutonic rocks of the Halmahera ophiolite, eastern Indonesia, an analogue of modern oceanic fore arcs. In: Parson, L.M., Murton, B.J., Browning, P. (Eds.), Ophiolites and their Modern Oceanic Analogues Special Publication 60. Geological Society, London, pp. 179–202.

Bloomer, S.H., 1983. Distribution and origin of igneous rocks from the landward slopes of the Mariana Trench, implications for its structure and evolution. Journal of Geophysical Research 88, 7411–7418.

Bonatti, E., Michael, P.J., 1989. Mantle peridotites from continental rifts to ocean basins to subduction zones. Earth and Planetary Science Letters 91, 297–311.

Brandon, A.D., Snow, J.E., Walker, R.J., Morgan, J.W., Morgan, J.W., Mock, T.D., 2000. ^{190}Pt–^{186}Os and ^{187}Re–^{187}Os systematics of abyssal peridotites. Earth and Planetary Science Letters 177, 319–335.

Bureau of Geology of Mineral Resources of Gansu Province (BGMRGP), 1989. Regional Geology of Gansu Province. Geological Publishing House, Beijing (in Chinese with English summary).

Bureau of Geology of Mineral Resources of Qinghai Province (BGMRQP), 1991. Regional Geology of Qinghai Province. Geological Publishing House Beijing (in Chinese with English summary).

Cannat, M., Bideau, D., Bougault, H., 1992. Serpentinised peridotites and gabbros in the Mid-Atlantic ridge axial valley at 15° 37′N and 16° 52′N. Earth and Planetary Science Letters 109, 87–106.

Chen, S.-M., 1996. A petrological and geochemical study of the ophiolitic rocks from Ayougou ophiolitic section, northwest Qilian fold belt. Unpublished MSc thesis, Cheng Kung University (in Chinese with English abstract).

Chung, C.-H., Smith, A.D., 2000. Nd–Sr isotopic and geochemical evidence on the tectonic setting of the Ta-Den Creek ophiolite, north Qilian fold belt, NW China. Journal of the Geological Society of China 43, 31–42.

Claesson, S., Pallister, J.S., Tatsumoto, M., 1984. Samarium–neodymium data on two late Proterozoic ophiolites of Saudi Arabia and implications for crustal and mantle evolution. Contributions to Mineralogy and Petrology 84, 244–252.

Dick, H.J.B., Bullen, T., 1984. Chromian spinel as a petrogenetic indicator in abyssal and Alpine-type peridotites and spatially associated lavas. Contributions to Mineralogy and Petrology 86, 54–76.

Edwards, R.L., Wasserburg, G.J., 1985. The age and emplacement of obducted oceanic crust in the Urals from Sm–Nd and Rb–Sr systematics. Earth and Planetary Science Letters 72, 389–404.

Elthon, D., 1992. Chemical trends in abyssal peridotites: refertilisation of depleted suboceanic mantle. Journal of Geophysical Research 97, 9015–9025.

Franz, L., Becker, K.-P., Kramer, W., Herzig, P.M., 2002. Metasomatic mantle xenoliths from the Bismarck microplate (Papua New Guinea)—thermal evolution, geochemistry and extent of slab-induced metasomatism. Journal of Petrology 43, 315–343.

Gruau, G., Bernard-Griffiths, J., Lécuyer, C., 1998. The origin of U-shaped rare earth patterns in ophiolite peridotites: assessing the role of secondary alteration and melt/rock reaction. Geochimica et Cosmochimica Acta 62, 3545–3560.

Hekinian, R., 1982. Petrology of the Ocean Floor, Oceanography Series 33. Elsevier, Amsterdam.

Hyndman, R.D., Peacock, S.M., 2003. Serpentinization of the fore arc mantle. Earth and Planetary Science Letters 212, 417–432.

Ito, E., White, W.M., Göpel, C., 1987. The O, Sr, Nd and Pb isotope geochemistry of MORB. Chemical Geology 62, 157–176.

Jacobsen, S.B., Wasserburg, G.J., 1979. Nd and Sr isotopic study of the Bay of Islands ophiolite complex and the evolution of the source of mid-ocean ridge basalts. Journal of Geophysical Research 84, 7429–7445.

Jacobsen, S.B., Quick, J.E., Wasserburg, G.J., 1984. A Nd and Sr isotopic study of the Trinity peridotite: implications for mantle evolution. Earth and Planetary Science Letters 68, 361–378.

Jacques, A.L., Chappell, B.W., 1980. Petrology and trace element geochemistry of the Papuan ultramafic belt. Contributions to Mineralogy and Petrology 75, 55–70.

Jahn, B.-M., Bernard-Griffiths, J., Charlot, R., Cornichet, J., Vidal, F., 1980. Nd and Sr isotopic compositions and REE abundance of Cretaceous MORB (Holes 417D and 418A Leg 51, 52 and 53). Earth and Planetary Science Letters 48, 171–184.

Janecky, D.R., Seyfried, W.E., 1986. Hydrothermal serpentinization of peridotite within the oceanic crust: experimental investigations of mineralogy and major element chemistry. Geochimica et Cosmochimica Acta 50, 1357–1378.

Jochum, K.P., Verma, S.P., 1996. Extreme enrichment of Sb, Tl and other trace elements in altered MORB. Chemical Geology 130, 289–299.

Johnson, L.E., Fryer, P., 1990. Petrography, geochemistry and petrogenesis of igneous rocks from the outer Mariana forearc. Earth and Planetary Science Letters 100, 304–316.

Lagabrielle, Y., Bideau, D., Cannat, M., Karson, J.A., Mével, C., 1998. Ultramafic–mafic plutonic rock suites exposed along the Mid-Atlantic Ridge (10°N–30°N). Symmetrical–asymmetrical distribution and implications for seafloor spreading processes. In: Buck, W.R., Delaney, P.T., Karson, J.A., Lagabrielle, Y. (Eds.), Faulting and Magmatism at Mid-Ocean Ridges Geophysical Monograph 106. American Geophysical Union, Washington, DC, pp. 153–176.

Li, X.-H., Zhao, J.-X., McCulloch, M.T., Zhou, G.-Q., Xing, F.-M., 1997. Geochemical and Sm–Nd isotopic study of Neoproterozoic ophiolites from southeastern China: petrogenesis and tectonic implications. Precambrian Research 81, 129–144.

Lin, Y.-T., 1997. A Petrological and Geochemical Study of the Ophiolitic Rocks from Chiutarn Temple of the Lhajyi Mountain, Qinghai province, NW China. Unpublished MSc thesis, Cheng Kung University (in Chinese with English abstract).

McCulloch, M.T., Gregory, R.T., Wasserburg, G.J., Taylor, H.P., 1981. Sm–Nd, Rb–Sr and $^{18}O/^{16}O$ isotope systematics in an oceanic crustal section: evidence from the Semail ophiolite. Journal of Geophysical Research 86, 2721–2735.

McDonough, W.F., 1990. Constraints on the composition of the continental lithospheric mantle. Earth and Planetary Science Letters 101, 1–18.

McInnes, B.I.A., Gregoire, M., Binns, R.A., Herzig, P.M., Hannington, M.D., 2001. Hydrous metasomatism of oceanic sub-arc mantle, Lihir, Papua New Guinea: petrology and geochemistry of fluid metasomatised mantle wedge xenoliths. Earth and Planetary Science Letters 188, 169–183.

Menzies, A.A., Long, A., Ingram, G., Tatnell, M., Janecky, D., 1993. MORB peridotite–sea water interaction: experimental constraints on the behaviour of trace elements, $^{87}Sr/^{86}Sr$ and $^{143}Nd/^{144}Nd$ ratios. In: Prichard, H.M., Alabaster, T., Harris, N.B.W., Neary, C.R. (Eds.), Magmatic Processes and Plate Tectonics Special Publication 76. Geological Society, London, pp. 309–322.

O'Hanley, D.S., 1996. Serpentinites: Records of Tectonic and Petrological History. Oxford University Press, New York.

Ohara, Y., Fujioka, K., Ishizuka, O., Ishii, T., 2002. Peridotites and volcanics from the Yap arc system: implications for tectonics of the southern Philippine Sea plate. Chemical Geology 189, 35–53.

Pearce, J.A., Lippard, S.J., Roberts, S., 1984. Characteristics and tectonic significance of supra-subduction zone ophiolites. In: Kokelaar, B.P., Howells, M.F. (Eds.), Marginal Basin Geology. Blackwell Scientific Press, Oxford, pp. 77–94.

Prinzhofer, A., Allègre, C.J., 1985. Residual peridotites and the mechanisms of partial melting. Earth and Planetary Science Letters 74, 251–265.

Rampone, E., Hofmann, A.W., Piccardo, G.B., Vannucci, R., Bottazzi, P., Ottolini, L., 1996. Trace element and isotope geochemistry of depleted peridotites from an N-MORB type ophiolite (Internal Ligurides N. Italy). Contributions to Mineralogy and Petrology 123, 61–76.

Scambelluri, M., Rampone, E., Piccardo, G.B., 2001. Fluid and element cycling in subducted serpentinite: a trace element study of the Erro-Tobbio high-pressure ultramafites (western Alps, NW Italy). Journal of Petrology 42, 55–67.

Sharma, M., Wasserburg, G.J., 1996. The neodymium isotopic compositions and rare earth patterns in highly depleted ultramafic rocks. Geochimica et Cosmochimica Acta 60, 4537–4550.

Sharma, M., Wassserburg, G.J., Papanastassiou, D.A., Quick, J.E., Sharkov, E.V., Laz'ko, E.E., 1995. High $^{143}Nd/^{144}Nd$ in extremely depleted mantle rocks. Earth and Planetary Science Letters 135, 101–114.

Shaw, H.F., Wasserburg, G.J., 1984. Isotopic constraints on the origin of Appalachian mafic complexes. American Journal of Science 284, 319–349.

Shaw, H.F., Chen, J.H., Saleeby, J.B., Wasserburg, G.J., 1987. Nd–Sr–Pb systematics and age of the Kings River ophiolite, California: implications for depleted mantle evolution. Contributions to Mineralogy and Petrology 96, 281–290.

Smith, A.D., Huang, L.-Y., 1997. The use of extraction chromatographic materials in procedures for the isotopic analysis of neodymium and strontium in rocks by thermal ionisation mass spectrometry. Cheng Kung Journal 32, 1–10.

Smith, A.D., Lambert, R.St.J., 1995. Nd, Sr, and Pb isotopic evidence for contrasting origins of Late Paleozoic volcanic rocks from the Slide mountain and Cache Creek terranes, south-central British Columbia. Canadian Journal of Earth Sciences 32, 447–459.

Smith, A.D., Fox, J.S., Farquhar, R., Smith, P., 1990. Geochemistry of Ordovician Køli Group basalts associated with Besshi-type Cu–Zn deposits from the southern Trondheim and Sulitjelma mining districts of Norway. Mineralium Deposita 25, 15–24.

Smith, A.D., Lian, F.-R., Chung, C.-H., Yang, H.-Y., 1997. Isotopic evidence from metasediments in the Qilian fold belt for a north China–Antarctica connection in the early Paleozoic. Journal of the Geological Society of China 40, 481–497.

Smith, A.D., Wen, D.-J., Huang, L.-Y., Wang, C.-S., 2000. Constraints from gneisses in the Qilian fold belt for the position of the north China block in the Proterozoic. Journal of the Geological Society of China 43, 81–93.

Snow, J.E., Hart, S.R., Dick, H.J.B., 1993. Orphan strontium-87 in abyssal peridotites: daddy was a granite. Science 262, 1861–1863.

Sun, S.-S., McDonough, W.F., 1989. Chemical and isotopic systematics of oceanic basalts: implications for mantle composition and processes. In: Saunders, A.D., Norry, M.J. (Eds.), Magmatism in the Ocean Basins Special Publication 42. Geological Society, London, pp. 313–345.

Tatsumi, Y., Eggins, S., 1995. Subduction Zone Magmatism. Blackwell Scientific Publications, Cambridge, MA.

Taylor, S.R., Gorton, M.P., 1977. Geochemical applications of spark-source mass spectrography, III. Element sensitivity, precision and accuracy. Geochimica et Cosmochimica Acta 41, 1375–1380.

Taylor, S.R., McLennan, S.M., 1985. The Continental Crust: Its Composition and Evolution. Blackwell, Oxford.

Thirlwall, M.F., Bluck, B.J., 1984. Sr–Nd isotope and chemical evidence that the Ballantrae 'ophiolite', SW Scotland, is polygenetic. In: Gass, I.G., Lippard, S.J., Shelton, A.W. (Eds.), Ophiolites and Oceanic Lithosphere. Blackwell Scientific Press, Oxford, pp. 215–230.

Tian, B., Wu, H.Q., 1994. Geochemistry of the two blueschist belts and implications for the early Paleozoic tectonic evolution of the north Qilian mountains, China. In: Wu, H.-Q., Tian, B., Liu, Y.Q. (Eds.), Very Low Grade Metamorphism: Mechanisms and Geological Applications. Seismological Press, Beijing, pp. 92–116.

Tseng, C.-Y., 1998. A petrological study of ophiolite from Baijing Temple of the North Qilian Mountains, Qinghai Province. Unpublished MSc Thesis, Cheng Kung University (in Chinese with English abstract).

Tseng, C.-Y., Yang, H.-Y., 2000. Mineralogy, petrology, and geochemical characteristics of the ophiolitic rocks in the vicinity of Baijing temple, north Qilian mountains, NW China. Journal of the Geological Society of China 43, 185–210.

Verma, S.P., 1992. Seawater alteration effects on REE, K., Rb, Cs, Sr, U, Th, Pb and Sr–Nd–Pb isotope systematics of mid-ocean ridge basalt. Geochemical Journal 26, 159–177.

Wan, Y.-S., Yang, J.-S., Xu, Z.-Q., Wu, C.-L., 2000. Geochemical characteristics of the Maxianshan complex and Xinglongshan group in the eastern segment of the Qilian orogenic belt. Journal of the Geological Society of China 43, 52–68.

Wu, H.Q., Feng, Y.-M., Song, S.G., 1993. Metamorphism and deformation of blueschist belts and their tectonic implications, north Qilian mountains, China. Journal of Metamorphic Geology 11, 523–536.

Xia, L., Xia, Z., Xu, X., 1996. Petrogenesis of Marine Volcanic Rocks from North Qilian Mountains. Geological Publishing House, Beijing (in Chinese).

Xiong, J., Coney, P.J., 1985. Accreted terranes of China. In: Howell, D.G. (Ed.), Tectonostratigraphic Terranes of the Circum-Pacific Region. Circum Pacific Council for Energy and Mineral Resources, Earth Science Series No.1, Houston, TX, pp. 349–361.

Xu, Z.-Q., Xu, H.-F., Zhang, J.-X., Li, H.-B., Zhu, Z.-Z., Qu, J.-C., Chen, D.-Z., Chen, J.-L., Yang, K.-C., 1994. The Zhoulangnanshan Caledonian subductive complex in the northern Qilian mountains and its dynamics. Acta Geologica Sinica 68, 1–15 (in Chinese with English abstract).

Xue, X., Baadsgaard, H., Irving, A.J., Scarfe, C.M., 1990. Geochemical and isotopic characteristics of lithospheric mantle beneath west Kettle river, British Columbia: evidence from ultramafic xenoliths. Journal of Geophysical Research 95, 15879–15891.

Zangana, N.A., Downes, H., Thirlwall, M.F., Marriner, G.F., Bea, F., 1999. Geochemical variation in peridotite xenoliths and their constituent clinopyroxenes from Ray Pic (French Massif Central): implications for the composition of the shallow lithospheric mantle. Chemical Geology 153, 11–35.

Zuo, G., Zhang, Z., Mao, J., Wu, M., Yang, J., Wang, Z., Zhang, Z., 2000. The age of ophiolite and tectonic framework of the western section of the north Qilian mountains, northwest China. Journal of the Geological Society of China 43, 43–51.